

# Parameter Identification of Static Friction Based on An Optimal Exciting Trajectory

X Tu, P Zhao and Y F Zhou\*

State Key Lab of Digital Manufacturing Equipment & Technology, Huazhong University of Science & Technology, Wuhan, Hubei, 430074, China

\* corresponding author, E-mai: yfzhou@hust.edu.cn

**Abstract.** In this paper, we focus on how to improve the identification efficiency of friction parameters in a robot joint. First, the static friction model that has only linear dependencies with respect to their parameters is adopted so that the servomotor dynamics can be linearized. In this case, the traditional exciting trajectory based on Fourier series is modified by replacing the constant term with quintic polynomial to ensure the boundary continuity of speed and acceleration. Then, the Fourier-related parameters are optimized by genetic algorithm(GA) in which the condition number of regression matrix is set as the fitness function. At last, compared with the constant-velocity tracking experiment, the friction parameters from the exciting trajectory experiment has the similar result with the advantage of time reduction.

## 1. Introduction

Friction is one of the most relevant problems to realize a successful feedback control in an industry robot[1, 2]. It exists in all mechanisms to some extent and appears to the function of the physical interface between two surfaces and greases in contact[3-7]. The nonlinear phenomenon physically resulting from the contact geometry, properties of materials, relative velocity, wears, ambient temperature, etc, may cause steady-state errors, limit cycling and system vibration[3]. In order to compensate the effect of friction in motion control, it is necessary to describe the frictional behavior. For this reason, many static friction models have been put forward.

The classical static friction models contain Coulomb friction and linear viscous damping, in which the friction is assumed as a function of velocity[8]. However, the property of stiction can't be adequately described. In literature [9], Morin introduced the situation where the starting friction is higher than friction at a nonzero velocity. Extra break-away forces are required to start the movement. In literature [10], the Stribeck effect that the friction force decreases continuously as intermediate velocity increasing for a certain velocity regime was observed. It was described by the Stribeck model

$$F_f = \begin{cases} F(\dot{\phi}) & (\dot{\phi} \neq 0) \\ F_e & (\dot{\phi} = 0, |F_e| < F_s) \\ F_s \cdot \text{sign}(F_e) & \text{otherwise} \end{cases} \quad (1)$$

Where  $F(\dot{\phi})$  for non-zero velocity describes the Stribeck, Coulomb, viscous friction as below,

$$F(\dot{\phi}) = F_c + (F_s - F_c)e^{-\left|\frac{\dot{\phi}}{v_s}\right|^\xi} + h(\dot{\phi}), \quad h(\dot{\phi}) = F_v \cdot \dot{\phi} \quad (2)$$



Where  $F_c, F_s, F_v$  are the coefficients of Coulomb friction, static friction, viscous friction, respectively and  $v_s$  is called Stribeck velocity. The term  $(F_s - F_c)\exp(-|\dot{\phi}/v_s|^\xi)$  describes the Stribeck phenomenon and tends to zero according to the speed  $v_s$  and exponent  $\xi$ . The term  $h(\dot{\phi})$  represents the viscous friction, which plays a heavy role at high speed. Obviously, the exponent term makes it impossible that the stibeck parameters are identified by linear predictors. In other words, friction has to be separated from other dynamic effects[11]. Indeed, an effective alternative is to use a third order polynomial function to represent both stibeck and coulomb phenomenons[2, 12]. It is also able to express the viscous effect that is not necessarily linear. Then the friction torque can be expressed as:

$$\tau_f(\dot{\phi}) = [c_0 + c_1|\dot{\phi}| + c_2|\dot{\phi}|^2 + c_3|\dot{\phi}|^3] \cdot \text{sign}(\dot{\phi}) \quad (3)$$

Where  $\dot{\phi}$  is the joint velocity and a symmetric function is also be considered. Similarly, literature [13] proposed a simplified model that is still capturing the downward bends and possible asymmetries while remaining linear in the unknown parameters. The model is the following:

$$\tau_f(\dot{\phi}) = [\alpha_0 + \alpha_1|\dot{\phi}|^{1/2} + \alpha_2|\dot{\phi}|] \cdot \text{sign}(\dot{\phi}) \quad (4)$$

It is noted that the parameters  $\alpha_i$  no longer represent dry friction or viscous damping but the sum of all effects of the multistage gears into a mathematical description[11]. It can be estimated by minimizing a least-square estimation algorithm.

Generally, the static model is adequate enough to describe the effects of friction, and the relevant coefficients can be easily achieved from the selecting parts of the measurement with constant velocity[14]. If only one joint is moved, the influence of centrifugal and Coriolis forces can be eliminated. A forward trajectory from  $\theta_1$  to  $\theta_2$  with constant-velocity is usually designed to acquire the real motor torque  $\tau_m^+$ , and reverse  $\tau_m^-$ . As the gravity torque  $\tau_g(\theta)$  is equal in both directions at the same joint angle  $\theta$ , we can obtain that

$$\tau_f(\dot{\theta}) - \tau_g(\theta) = \tau_m^+, \quad \tau_f(-\dot{\theta}) - \tau_g(\theta) = \tau_m^- \quad (5)$$

Subtracting the equations above yields:

$$\tau_f(\dot{\theta}) - \tau_f(-\dot{\theta}) = \tau_m^+ - \tau_m^- \quad (6)$$

Since the friction forces in both directions are approximate, i.e.  $\tau_f(\dot{\theta}) \approx -\tau_f(-\dot{\theta})$ , then a direction-independent estimate of friction and gravity can be achieved as:

$$\tau_f(\dot{\theta}) = (\tau_m^+ - \tau_m^-) / 2, \quad \tau_g(\theta) = -(\tau_m^+ + \tau_m^-) / 2 \quad (7)$$

Obviously, in this way Multi- repetitive works, especially the friction samplings at an ultra low speed, will make the parameter identification so inefficiency. In order to evaluate the friction coefficients by moving the joint at one time and guarantee the friction accuracy, an optimal periodic trajectory is designed to minimize the condition numbers of observation matrix, which is from the linear dynamic model of the servomotor. The paper is organized as follows. Sect.2 presents the linear predictors of joint friction and an excitation trajectory based on periodic Fourier series with its boundary optimization. Sect. 3 contains the process of friction identification experiment with designed trajectory and the comparison with the constant-speed tracking experiment. Last, conclusions are presented in Sect.4.

## 2. Static friction model and parameter identification

### 2.1 the linearization of single joint system

For a robot, since each joint can be considered as a one degree-of-freedom(DOF) system, the dynamic of the joint system can be described as[2]:

$$J\ddot{\theta} = \tau_m - \tau_f + \tau_g \quad (8)$$

Where  $J$  is the nominal inertia(motor plus charge),  $\beta$  is the angular acceleration of the motor,  $\tau_m$  is the motor torque,  $\tau_f$  is the friction torque scalar and  $\tau_g$  is the gravity torque of joint, which is the function of joint position and expressed as below:

$$\tau_g = p_x \cos(q) - p_y \sin(q) \quad (9)$$

Where  $p_x, p_y$  are called gravity observation coefficient,  $q$  is the joint angle. We select equation (4) as the static friction model. In this case, a standard least-squares method can be applied to estimate the friction coefficients. According to equation (4), equation (8) and equation (9), the motor torque in the motor side can be rewritten as:

$$\tau_m = m\phi \quad (10)$$

Where the vector

$$\phi = [J, \alpha_0, \alpha_1, \alpha_2, p_x, p_y]^T \quad (11)$$

The observation vector

$$m = [\beta, \text{sign}(\dot{q}), \text{sign}(\dot{q})|\dot{q}|^{0.5}, \text{sign}(\dot{q})|\dot{q}|, -\cos(q), \sin(q)] \quad (12)$$

and then vector  $m$  can be written in matrix form where all the samples are collected along a specific trajectory. Then,

$$\hat{\tau}_m = M\phi \quad (13)$$

where

$$\hat{\tau}_m = [\tau_1, \tau_2, \tau_3, \dots, \tau_k]^T \quad (14)$$

is the vector of measured motor torque at  $k$  sampling times. The observation matrix

$$M = \begin{bmatrix} \beta_1 & \text{sign}(\dot{q}_1) & \text{sign}(\dot{q}_1)|\dot{q}_1|^{0.5} & \text{sign}(\dot{q}_1)|\dot{q}_1| & -\cos(q_1) & \sin(q_1) \\ \beta_2 & \text{sign}(\dot{q}_2) & \text{sign}(\dot{q}_2)|\dot{q}_2|^{0.5} & \text{sign}(\dot{q}_2)|\dot{q}_2| & -\cos(q_2) & \sin(q_2) \\ \vdots & \vdots & \vdots & \vdots & \vdots & \vdots \\ \beta_k & \text{sign}(\dot{q}_k) & \text{sign}(\dot{q}_k)|\dot{q}_k|^{0.5} & \text{sign}(\dot{q}_k)|\dot{q}_k| & -\cos(q_k) & \sin(q_k) \end{bmatrix} \quad (15)$$

contains the motion data measured with an exciting trajectory. In this case, the coefficients are estimated by the use of the LS technique as

$$\phi = M^+ \hat{\tau}_m \quad (16)$$

where  $M^+$  is the pseudo-inverse of the matrix  $M$ .

## 2.2 the design and optimization of exciting trajectory

The measurement noise and uncertainty of model can result in the deviation of parameter identification[15]. An excellent trajectory can greatly improve the identification precision and anti-noise capacity. Obviously, the trajectory needs to span all the joint velocities for many times in order to reduce the measurement noise and excite all the friction dynamics. If one or more parameters are not excited, the matrix  $M$  loses its full rank and equation (16) cannot be solved. Swevers [16, 17] etc. choose a finite Fourier series to be the exciting trajectory for each joint, which has the advantages of convenient data processing and insensitivity to noise. However, the Fourier series does not meet the boundary conditions of velocity and acceleration. In the beginning and end of the movement in a period, the mutations of velocity will lead to the joint vibration and reduce the parameter identification precision. Therefore, we add a quintic polynomial instead of the constant term in the Fourier series to ensure the continuity of the trajectory boundary. The improved Fourier series is written as

$$\begin{aligned}
q(t) &= \sum_{l=1}^N \frac{a_l}{\omega_f l} \sin(\omega_f l t) - \frac{b_l}{\omega_f l} \cos(\omega_f l t) + \sum_{k=0}^5 c_k (t - (j-1)t_f)^k \\
t_f &= 2\pi / \omega_f \\
j &= \begin{cases} 1 & \text{if } t = 0 \\ \text{ceil}(t / t_f) & \text{else} \end{cases} \\
\dot{q}(t) &= \sum_{l=1}^N a_l \cos(\omega_f l t) + b_l \sin(\omega_f l t) + \sum_{k=1}^5 c_k \cdot k \cdot (t - (j-1)t_f)^{k-1} \\
\ddot{q}(t) &= \sum_{l=1}^N -a_l \cdot (\omega_f l) \cdot \sin(\omega_f l t) + b_l \cdot (\omega_f l) \cdot \cos(\omega_f l t) + \sum_{k=2}^5 c_k \cdot k \cdot (k-1) \cdot (t - (j-1)t_f)^{k-2}
\end{aligned} \tag{17}$$

Where  $t_f$  is the period of trajectory,  $\omega_f$  is called the fundamental frequency,  $N$  means the number of the harmonic waves,  $a_l, b_l (l=1, 2, \dots, N)$ ,  $c_k (k=1, 2, \dots, 5)$  are constant coefficients. In order to ensure that the robot can accurately track the exciting trajectory, we set the boundary condition as two part as below: the equality constraint,

$$q(0) = q_0, \quad q(t_f) = q_0, \quad \dot{q}(0) = 0, \quad \dot{q}(t_f) = 0, \quad \ddot{q}(0) = 0, \quad \ddot{q}(t_f) = 0 \tag{18}$$

the inequality constraint,

$$q_{\min} \leq q(t) \leq q_{\max}, \quad \dot{q}_{\min} \leq \dot{q}(t) \leq \dot{q}_{\max}, \quad \ddot{q}_{\min} \leq \ddot{q}(t) \leq \ddot{q}_{\max} \tag{19}$$

where  $q_{\min}, \dot{q}_{\min}, \ddot{q}_{\min}, q_{\max}, \dot{q}_{\max}, \ddot{q}_{\max}$  are the minimum or maximum values of joint angle, speed and acceleration, respectively. Combining the equations from (17) to (19), we can derive the matrix expression of boundary constraint as below,

$$\begin{bmatrix} q_0 \\ q_{t_f} \\ \dot{q}_0 \\ \dot{q}_{t_f} \\ \ddot{q}_0 \\ \ddot{q}_{t_f} \end{bmatrix} = \begin{bmatrix} 0 & 0 & 0 & 0 & 0 & 1 \\ t_f^5 & t_f^4 & t_f^3 & t_f^2 & t_f & 1 \\ 0 & 0 & 0 & 0 & 1 & 0 \\ 5t_f^4 & 4t_f^3 & 3t_f^2 & 2t_f & 1 & 0 \\ 0 & 0 & 0 & 2 & 0 & 0 \\ 20t_f^3 & 12t_f^2 & 6t_f & 2 & 0 & 0 \end{bmatrix} \begin{bmatrix} c_5 \\ c_4 \\ c_3 \\ c_2 \\ c_1 \\ c_0 \end{bmatrix} + \begin{bmatrix} s_0 \\ s_1 \\ s_2 \\ s_3 \\ s_4 \\ s_5 \end{bmatrix} \tag{20}$$

where

$$s_0 = \sum_{l=1}^N -\frac{b_l}{\omega_f l}, \quad s_1 = s_0, \quad s_2 = \sum_{l=1}^N a_l, \quad s_3 = s_2, \quad s_4 = \sum_{l=1}^N b_l \omega_f l, \quad s_5 = s_4 \tag{21}$$

and

$$c_0 = q_0 + \sum_{l=1}^N \frac{b_l}{\omega_f l}, \quad c_1 = -\sum_{l=1}^N a_l, \quad c_2 = -\frac{1}{2} \sum_{l=1}^N b_l \omega_f l, \quad c_3 = -\frac{2c_2 t_f + 10c_1}{t_f^2}, \quad c_4 = \frac{15c_1 + c_2 t_f}{t_f^3}, \quad c_5 = \frac{-6c_1}{t_f^4} \tag{22}$$

Obviously, the multinomial coefficients  $c_i (i=0, 1, \dots, 5)$  can be seen as the function of  $a_l$  and  $b_l$  so that the number of Fourier parameters to be optimized has been reduced.

Generally, the random noises mixed in motion and torque samples have a bad effect on identification precision. In order to strengthen the anti-noise ability and robustness of the model (13), the Fourier parameters should be optimized. Since the condition number of the regression matrix  $M$  reflects the performance of the exciting trajectory, the optimization criteria can be expressed as,

$$\min \text{cond}(M) \Big|_{a_l, b_l} \tag{23}$$

Combining with the limits for each joint position, speed, and acceleration (seen in equation (18),(19)), we can adopt genetic algorithm (GA) to solve the problem of nonlinear constrained optimization.

In the GA, the Fourier parameter  $N$  is set as 5, and the coefficients of exciting trajectory are set as genetic populations, i.e.,

$$x = [a_1, a_2, \dots, a_5, b_1, b_2, \dots, b_5] \tag{24}$$

equation (23) is taken as the individual fitness function. The random sampling selection method is adopted for the best individual who is coded by decimal floating point coding method. The crossover probability is set as 0.9. For mutation operation, we select the Gauss mutation operator whose mutation probability is self-adjusted with the process of evolution. It can be expressed as,

$$p_m = (p_{mo} - (p_{mo} - p_{mmin}) \cdot \frac{g}{G}) \quad (25)$$

where  $p_{mo}$  is the initial mutation probability,  $p_{mmin}$  is the minimum probability,  $g$  is the current hereditary time,  $G$  is the maximum hereditary time and set as 100.

### 3. Experiment of friction parameter identification

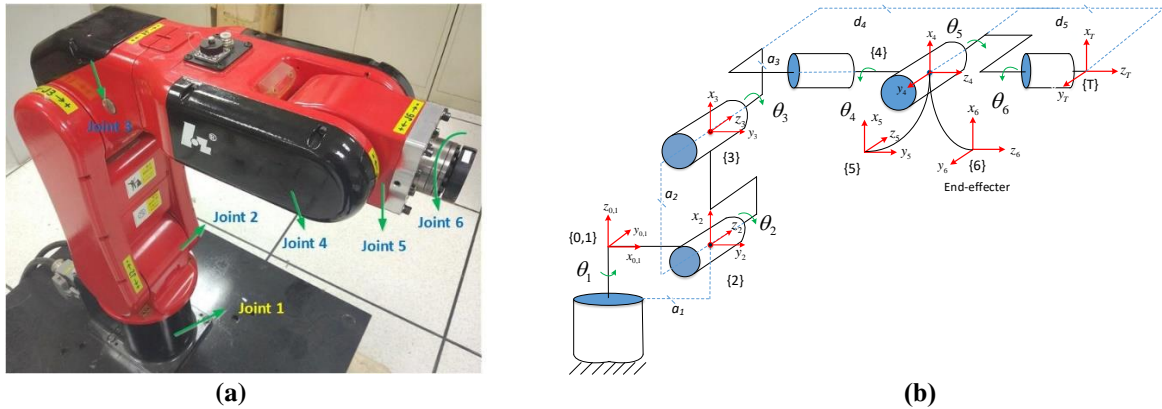


**Figure.1** The experiments were made in joint 4 of HSR robot. (a) the robot used in the experiments; (b) Modified D-H coordinate system.

In this paper, all the experiments are made in joint 4 of Robot HSR-JR605-C as seen in figure 1, and the kinematic parameters are listed in **Table 1**.

**Table 1.** Kinematic parameters of joint 4.

| $\theta_4$<br>(deg) | $\dot{\theta}_4$<br>(deg/s) | $\ddot{\theta}_4$<br>(deg/s <sup>2</sup> ) | <i>Jerk</i><br>(deg/s <sup>3</sup> ) | (max) <i>Gear Ratio</i><br>( $\eta$ ) |
|---------------------|-----------------------------|--|--------------------------------------|---------------------------------------|
| [-180,180]          | [-40,40]                    | [-500,500]                                 | [-45000,45000]                       | 76.5:1                                |
| $t_f$ (s)           | $\omega_f$                  | <i>Sampling rate</i> (Hz)                  | $q_0$ (degree)                       | <i>Rated current</i><br>(A)           |
| 3                   | $2\pi/3$                    | 500  | 0                                    | 2.546                                 |

In this case, we derive the Fourier coefficients by GA method as  $a_1 = 0.6340, a_2 = 0.0160, a_3 = -0.0032, a_4 = 0.0072, a_5 = 0.0072, b_1 = 0.4397, b_2 = -0.0194, b_3 = -0.14525, b_4 = -0.0697, b_5 = 0.0731$ . Based on the TwinCAT platform, an optimal trajectory tracking experiment(OTTE) is designed. we move the joint 4 along the optimal trajectory and sample the movement and motor torque for  $N(N=50)$  periods. At the same time, all the other axes keep the initial posture, i.e.,  $[\theta_1, \theta_2, \theta_3, \theta_5, \theta_6] = [0, -\pi/2, 0, 0, 0]$ . In order to improve the signal-to-noise ratio(SNR) of the sampling date, an average method in time domain is chosen as below,

$$\hat{q}(k) = \frac{1}{N} \sum_{i=1}^N q_{4i}(k), \quad \hat{\dot{q}}(k) = \frac{1}{N} \sum_{i=1}^N \dot{q}_{4i}(k), \quad \hat{\ddot{q}}(k) = \frac{1}{N} \sum_{i=1}^N \ddot{q}_{4i}(k), \quad \hat{\tau}(k) = \frac{1}{N} \sum_{i=1}^N \tau_{4i}(k) \quad (26)$$

Where  $k$  represents the  $k$ th sampling in a cycle and  $q_{4i}(k), \dot{q}_{4i}(k), \ddot{q}_{4i}(k), \tau_{4i}(k)$  means the angle, speed, acceleration and motor torque of joint 4 in  $k$ th sampling and  $i$ th period, respectively. Moreover,

to further improve the quality of measured signals, a high-speed nonlinear discrete tracking-differentiator(HSTD)[18] is adopted to clean the noise of the position and torque signals, and then its first and second order derivatives can be derived. The results are shown in figure 2:

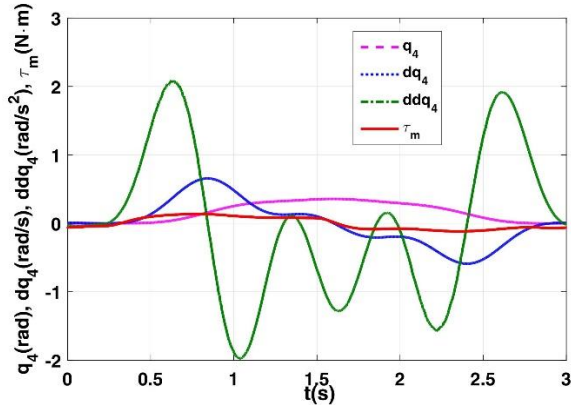


**Figure. 2** Measured signals of position, speed, acceleration and motor torque of joint 4 along the exciting trajectory.

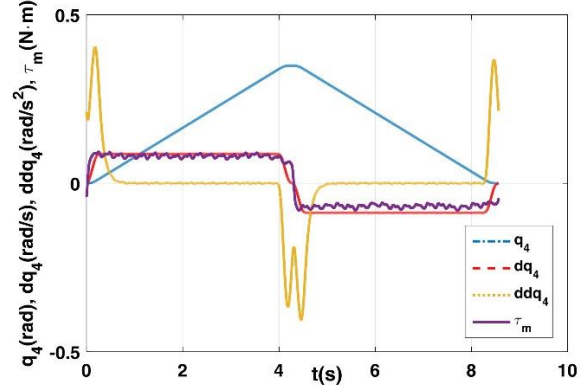


**Figure. 3** Measured movement along a constant-speed trajectory

In this case, the speed is normalized and the parameter vector  $\phi$  can be achieved according to equation (16) as  $\phi=[0.0001887,0.087,-0.141,0.35,0.022087,0.132585]$ , then the friction parameters are obtained. In order to ascertain the validity of the identification results, the constant-velocity tracking experiments (CVTE) are made for comparison.

we select S wave (seen in figure 3) that traverses the constant-speed trajectory region  $[20:70]\text{deg}$  to acquire different joint angle mapping 29 sets of speed samples from 0 to  $30\text{deg/s}$  in the joint side. Obviously, it takes a long time to move at an ultra-low speed. For reducing the impact of random noise, joint 3 is moved periodically at 50 times. In this case, based on equation (7), the results of the friction-velocity wave can be figured as below:

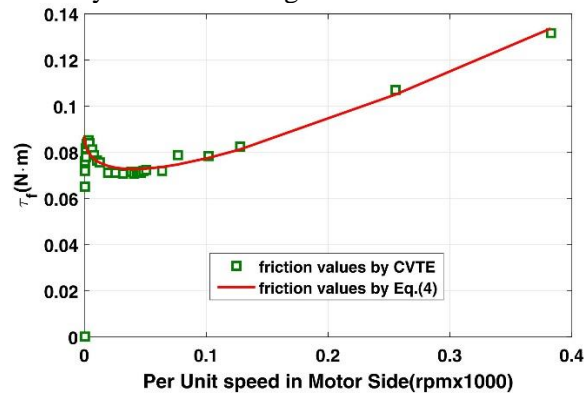


**Figure. 4** Friction-velocity waves by CVTE and OTTE

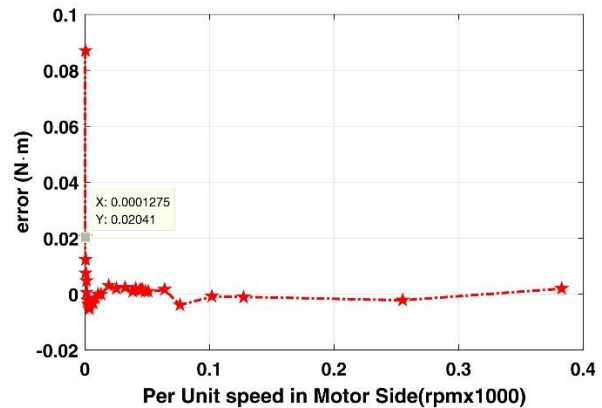


**Figure. 5** The error values of friction to different velocities.

From the figure 4&5, we can derive that the results of those different experiments have a great similarity. Obviously, relatively large errors occur at low speeds, but fewer errors exist at higher speeds. In general applications, the friction parameter identification with an optimal trajectory can be adopted because of the good description of the measured characteristics.

#### 4. Conclusion

In this paper, we take an exciting trajectory to identify the static friction parameters instead of the traditional constant-velocity trajectory. The Fourier series has been taken to build the period trajectory, in which the constant term is replaced by a quintic polynomial to meet the speed and acceleration's



boundary condition of continuity. In this case, the GA is used to get the trajectory to satisfy the constraints and not sensitive to the measurement noise. On this condition, only one tracking trajectory is necessary to take the place of the multi-tracking experiments, thus the identification efficiency is greatly improved.

### Acknowledgments

Research supported by National Natural Science Foundation of China (Project number: 51375194 and 51575411) and State Key Lab of Digital Manufacturing Equipment & Technology, School of Mechanical Science and Engineering, Huazhong University of Science & Technology.

### Reference

- [1] Guillo M, Dubourg L 2016 Impact & improvement of tool deviation in friction stir welding: Weld quality & real-time compensation on an industrial robot *Robotics&Computer-Integrated Manufacturing* **39** 22-31
- [2] Simoni L, Beschi M, Legnani G, et al. 2015 Friction modeling with temperature effects for industrial robot manipulators *IROS. IEEE/RSJ International Conference on. IEEE* 3524-3529
- [3] Bittencourt A C, Axelsson P 2014 Modeling and experiment design for identification of wear in a robot joint under load and temperature uncertainties based on friction data *IEEE-Asme Transactions On Mechatronics* **19**(5) 1694-1706
- [4] Bittencourt A C, Gunnarsson S 2012 Static friction in a robot joint—modeling and identification of load and temperature effects *Journal of Dynamic Systems, Measurement, and Control* **134**(5) 51013
- [5] Marton L, Lantos B. 2011 Control of robotic systems with unknown friction and payload *IEEE Transactions on Control Systems Technology* **19**(6) 1534-1539
- [6] Bittencourt A C, Axelsson P, Jung Y, et al. 2011 Modeling and identification of wear in a robot joint under temperature uncertainties *IFAC Proceedings Volumes* **44**(1) 10293-10299
- [7] Freidovich L, Robertsson A, Shiriaev A, et al. 2010 Lugre-model-based friction compensation *IEEE Transactions on Control Systems Technology* **18**(1) 194-200
- [8] Olsson H, Åström K J, Canudas De Wit C, et al. 1998 Friction models and friction compensation *European Journal of Control* **4**(3) 176-195
- [9] Morin A J 1833 New friction experiments carried out at metz in 1831 - 1833 *Proceedings of the French Royal Academy of Sciences* **4**(1) 128
- [10] Stribeck R 1902 The key qualities of sliding and roller bearings *Zeitschrift des Vereines Deutscher Ingenieure* **46**(38) 39
- [11] Grotjahn M, Daemi M, Heimann B 2001 Friction and rigid body identification of robot dynamics *International Journal of Solids and Structures* **38**(10) 1889-1902
- [12] Visioli A, Legnani G 2002 On the trajectory tracking control of industrial scara robot manipulators *IEEE transactions on industrial electronics* **49**(1) 224-232
- [13] Canudas De Wit C, Noel P, Aubin A, et al 1991 Adaptive friction compensation in robot manipulators: low velocities *The International Journal Of Robotics Research* **10**(3) 189-199
- [14] Liu G, Goldenberg A A, Zhang Y 2004 Precise slow motion control of a direct-drive robot arm with velocity estimation and friction compensation *Mechatronics* **14**(7) 821-834
- [15] Van Geffen V 2009 A study of friction models and friction compensation *DCT* **118** 24
- [16] Swevers J, Ganseman C, De Schutter J, et al. 1996 Experimental robot identification using optimised periodic trajectories *Mechanical Systems and Signal Processing* **10**(5) 561-577
- [17] Swevers J, Ganseman C, Tukul D B, et al. 1997 Optimal robot excitation and identification *IEEE transactions on robotics and automation* **13**(5) 730-740
- [18] Xie Y, Long Z 2009 A high-speed nonlinear discrete tracking-differentiator with high precision *Control Theory & Applications* **26**(2) 127-132